International Journal of Design & Nature and Ecodynamics
Vol. 20, No. 5, May, 2025, pp. 957-966
Journal homepage: http://iieta.org/journals/ijdne

Identification of Functional Groups, Mineral, and Oxide Composition of Geo-Biomaterials for Soil Amelioration

Teguh Budi Prasetyo[1], Amsar Maulana[2], Mimien Harianti[1], Indra Dwipa[3], Herviyanti Herviyanti[1*]

[1] Department of Soil Science and Land Resources, Agriculture Faculty, Andalas University, Padang City 25164, Indonesia
[2] Agriculture Faculty, Andalas University, Padang City 25164, Indonesia
[3] Department of Agronomy, Agriculture Faculty, Andalas University, Padang City 25164, Indonesia

Corresponding Author Email: herviyanti@agr.unand.ac.id

https://doi.org/10.18280/ijdne.200501

Received: 15 January 2025
Revised: 18 May 2025
Accepted: 23 May 2025
Available online: 31 May 2025

Keywords:
Ameliorant, Biochar, FT-IR, NaOH, Sub-bituminus coal, XRD, XRF

ABSTRACT

Ameliorant formulations derived from geo-biomaterials using amelioration technology have the potential to function as soil improvers, fertilizers, and adsorbents for controlling farmland pollution and improving soil and crop quality. This research identified the functional groups, mineral content, and oxide composition of geo-biomaterial-based ameliorant formulations, including sub-bituminous coal (SC), sub-bituminous coal activated with NaOH (A-SC), and biochar derived from young coconut waste (B-YCW). The study used two types of ameliorant formulations (FA), namely FA.a (SC + B-YCW) and FA.b (A-SC + B-YCW), each applied in three mixing ratios (75:25, 50:50, and 25:75) within a completely randomized design (CRD) with three replications. The study identified various functional groups (e.g., hydroxyls, amines, alkyls, terminal alkynes and alkenes, alkynes, nitriles carbonyls and minerals (e.g., quartz, muscovite, magnetite, and ulvospinel), along with oxide components such as P_2O_5, K_2O, SO_3, CaO, MgO, ZnO, CuO, MnO, SiO_2, Cl, Fe_2O_3, and Al_2O_3 in the geo-biomaterial formulations. The formulations containing 25% SC + 75% B-YCW and 25% A-SC + 75% B-YCW exhibited reduced transmittance corresponding to the stretching vibrations of C–H bonds (e.g., –C≡C–H, C=C–H), indicating a reduction or shift of these functional groups. In the 25% SC + 75% B-YCW formulation, the CaO content increased from 6.23% to 28.46%. In the 25% A-SC + 75% B-YCW formulation, K_2O increased from 20.51% to 45.65%, SO_3 from 0 to 3.58%, CaO from 13.85% to 23.03%, CuO from 0.08% to 0.13%, and Cl from 1.84% to 5.59%, compared to other formulations. Therefore, the formulations consisting of 25% SC + 75% B-YCW or 25% A-SC + 75% B-YCW are recommended as effective soil ameliorants based on their chemical and functional characteristics.

1. INTRODUCTION

Land and soil degradation due to intensive agricultural activities, deforestation, excessive use of synthetic chemicals, and land use change have become crucial issues in the environmental and agricultural sectors. Degraded soils not only lose their fertility but also have a reduced capacity to store water, retain nutrients, and support soil microorganisms that are essential for plant growth [1, 2]. The development of amelioration technology is an important strategy to restore the productivity of degraded agricultural soils and improve soil quality, forming the foundation for the sustainable development of geo-biomaterials. One promising approach to soil amelioration is the utilization of geo-biomaterials, which are mineral and biomass-based materials derived from natural resources or modified organic and inorganic wastes. However, the effectiveness of geo-biomaterials is largely determined by their chemical composition and functional structure, including the presence of functional groups, mineral content, and oxide composition. Sub-bituminous coal (SC), in powder form and chemically activated with alkaline materials, along with optimized biomass-derived biochar, presents promising opportunities as geo-biomaterials for soil amelioration and soil quality improvement.

The use of SC as a soil ameliorant is based on its high humic substance (HS) content of 31.5%, consisting of 21% humic acid (HA) and 10.5% fulvic acid (FA), extracted using 0.5 N NaOH [3-5]. SC is chemically activated to break hydrocarbon bonds or oxidize surface molecules, thereby altering both physical and chemical properties, such as increasing surface area and adsorption capacity. Chemical activation is chosen and recommended because it tends to be easier and more effective in its application in the field. Activators used in the chemical activation of SC include NaOH, NaCl, urea, KCl, and various forms of limestone such as CaO, $Ca(OH)_2$, $CaCO_3$, and $CaMg(CO_3)_2$ [6-8]. Extraction methods using NaOH, KOH, and sodium pyrophosphate have been applied to peat. NaOH and KOH were more effective in releasing humic substances from Sphagnum peat, while sodium pyrophosphate was more effective on Carex peat [9, 10]. Meanwhile, the addition of KOH increases the extraction yield and the amount of components such as K, Fe, and N in HA, which is advantageous for humic fertilizer applications [11, 12]. The A-SC is the best activation in improving SC chemical properties such as pH (5.34-12.65), CEC (24.39-148.20 cmolc kg^{-1}), and increasing the number of functional groups O-H, C=O, and CH_3. In addition, it can also improve the chemical properties of Ultisols such as pH, CEC, organic C, available P, and total N respectively by 1.49, 28.08 cmolc kg^{-1}, 1.63% C, 2.37 ppm P, 0.06% N, and reduce Al-exch by 1.17 cmolc kg^{-1}, and sodium adsorption ratio (SAR) by 0.03% and exchangeable sodium percentage (ESP) by 0.82%, compared to the control [13]. The potential and use of SC has been explored, but to increase its SC in formulation with biochar as a soil improver needs to be developed.

Biochar, as one type of ameliorant, is very promising, as its production from organic waste is cost-effective, and can fertilize the soil and reduce the solubility of heavy metals in the soil. The pyrolysis of agricultural organic waste produces biochar, a carbon-rich substance. Still, different raw materials, pyrolysis temperatures, and methods, and their functionalization require testing to identify the morphology and characteristics of biochar. One of the potential organic wastes that can be used is young coconut waste (YCW). The potential of YCW is very large because it is easily available, and its utilization also contributes to reducing the impact of environmental pollution from organic waste. According to the Environmental Agency, Padang City in 2019, young coconut waste reached 7 tons every day in Padang City. Based on this potential, young coconut waste can be carbonized with a yield of 20.87% into biochar or around 1.4 tons through the principle of pyrolysis in the Kon-Tiki method [14, 15]. The addition of 2% B-YCW an increase pH, available P, organic C, and CEC by 1.09, 1.70 ppm, 0.99%, and 9.12 cmolc kg^{-1}, respectively, and reduce Al-exch (3.19 cmolc kg^{-1}) to unmeasurable, compared to 0% biochar [16]. This presents a new opportunity for young coconut fruit waste biochar as an ameliorant formulation with sub-bituminous coal to improve soil and crop productivity.

The identification of functional groups, minerals, and oxide composition in geo-biomaterials is very important to ensure their potential and effectiveness and the utilization of SC, A-SC, and B-YCW as soil amendments, fertilizers, and adsorbents for the removal of pollutants such as pesticides and heavy metals on agricultural land. This is a new opportunity to develop potential strategies for geo-biomaterials that can be sustainably applied in amelioration technologies to improve soil and crop productivity, and also support the application of sustainable nature-based solutions to address soil degradation. This research identified the functional groups, minerals, and oxide composition of geo-biomaterials for their application as soil ameliorants.

2. MATERIALS AND METHODS

This research will be carried out at the Laboratory of Chemistry and Soil Fertility, Department of Soil Science and Land Resources, Faculty of Agriculture, Andalas University (UNAND), Padang, West Sumatra, Indonesia. Analysis of FT-IR, XRD, and XRF at the Laboratory of Chemical and Physics, Faculty of Mathematics and Natural Science, and the Integrated Laboratory, State University of Padang (UNP), Padang, West Sumatra, Indonesia, starting from July to November 2024.

2.1 Experimental design

Ameliorant formulation (FA) research consists of two types of combinations and three formulations in a completely randomized design (CRD) with three replications (Table 1).

Table 1. Ameliorant formulation of geo-biomaterial

Code			Treatments
FA.a	1	75% SC + 25% B-YCW	Sub-bituminous coal and young coconut waste biochar
	2	50% SC + 50% B-YCW	
	3	25% SC + 50% B-YCW	
FA.b	1	75% A-SC + 25% B-YCW	Activation of sub-bituminous coal with NaOH and young coconut waste biochar
	2	50% A-SC + 50% B-YCW	
	3	25% A-SC + 50% B-YCW	

2.2 Materials

2.2.1 Sub-bituminous coal

The SC was collected from Bonjol Pasaman, West Sumatra, at a depth of 1-2 meters from the ground soil. It was cleaned, smoothed with a Disc Mill type FFC 23, then sieved with a 500µm Electromagnetic Sieve Shaker EMS-8 for 10 minutes.

2.2.2 Activation of sub-bituminous coal with 10% NaOH

The SC is weighed depending on the formulation's dose and % (sample weight). The SC is activated by dissolving 10% NaOH in H_2O based on the SC's field capacity, as given in Eq. (1).

$$10\% \text{ NaOH (g)} = \frac{10}{100} \times \text{coal weight} \quad (1)$$

In addition, the mixture is uniformly mixed, left to stand for 1×24 hours in a 250 mL beaker, and covered with aluminium foil and a plastic covering. To homogenize the water content in the ameliorant, the A-SC findings are dried in an oven at 40-70℃ for 24 hours [13].

2.2.3 Biochar production from young coconut waste

The young coconut waste (*Cocos nucifera* L.) was chopped into ±10×5 lengths and dried for 7 days at Andalas University's Greenhouse Faculty of Agriculture, reaching 18.20% moisture. Furthermore, biochar is produced utilizing the Kon-Tiki technique, which consists of a conical steel with a top diameter of 100 cm, a height of 90 cm, a wall slope of 63.50°, and a capacity of 827 liters. The pyrolysis products were sprayed with water to stop the combustion process, then dried in an oven at 40-70℃ for 48 hours to achieve uniform biochar moisture content. Biochar particle size was separated using an Electromagnetic Sieve Shake EMS-8 on a 500µm sieve [14, 15, 17, 18]. The next step is to analyze the characteristics of biochar in the laboratory [19].

2.3 Geo-biomaterial

The formulation of the ameliorant was determined on a trial basis as a 100% ameliorant formulation. The FA is determined by the water retention capacity of each ameliorant utilized. The ameliorant formulations were carried out according to the treatment dose (Table 1 and Figure 1), and then homogenized in a 100 mL beaker using a shaker at 300 rpm for 30 minutes, and H_2O was added depending on each ameliorant's field capacity. The formulation was dried in an oven at 40-70°C for 1×24 hours. In addition, the ameliorant formulation was examined in the laboratory [19].

2.4 Analysis of geo-biomaterial by FT-IR, XRD, and XRF

Fourier transform infrared (FT-IR) spectra were measured over the spectral range between 485 to 8,500 cm^{-1} using an ABB MB-3000 series FTIR spectrometer instrument with a diamond internal reflection element (IRE) in absorbance mode. Resolution from 0.7 cm^{-1} with apodization resolution adjustable from 1 to 64 cm^{-1}, in 2 cm^{-1} increments, and a signal-to-noise ratio (S/N) of about 50,000:1 (root-mean-square, 60 s, 4 cm^{-1}, at peak response). Signal sampling by 24-bit ADC, short-term stability < 0.09%, temperature stability < 1% per °C with frequency repeatability (@ 1918 cm^{-1}) < 0.001 cm^{-1} and frequency accuracy (@ 1918 cm^{-1}) < 0.06 cm^{-1}.

X-ray diffraction (XRD) was used to determine the mineral composition of the ameliorant samples and formulations. The equipment used was a Philips PANalytical instrument with a PW 3830 X-ray generator operating at an operating voltage range of 20-60 kV (40 kV) and an operating current range of 20-100 mA (25 mA) with a Copper (Cu) anode producing Cu Kα radiation. The X-ray tube was sealed with a long fine focus (LFF) with a maximum power of 6 kW. The powder samples were oven dried for 12 hours at 100°C to remove absorbed water using an alcohol spatula, The samples were squeezed into a rectangular aluminium sample holder, which was then clamped onto the instrument sample holder. The sample was scanned in 0.02 increments from a theta scale of 5 to 85 degrees 2 and counted for 0.5 seconds per step.

X-ray fluorescence (XRF) equipment with an element range from sodium (Na) to uranium (U) and having Rhodium (Rh) standard anode, maximum voltage 30 kV, maximum current 0.1 mA, maximum power 9W on 2.4 kW X-ray tube. The detector has a high-resolution silicon drift detector (SDD) with an energy resolution of approximately 160 eV at the Kα Manganese line (5.9 keV) and a maximum count rate of 7,000 counts per second.

3. RESULTS AND DISCUSSION

The ameliorant formulation produced from the ameliorant shows color differences in the composition and percentage of ameliorants carried out. The ameliorant composition consists of two different compositions, namely SC + B-YCW and A-SC + B-YCW. The percentage of ameliorants combined consists of three, namely (1) 75% + 25%; (2) 50% + 50%, and (3) 25% + 75% (Figure 1). Colors were identified with the soil Munsell color chart. The color identified in the first composition shows that the higher the percentage of BS, the grayer and the darker, with the decrease in the percentage of SC or the increase in the percentage of B-YCW, namely 5Y 4/2 (grayish olive) and 5Y 2/2 (olive black). Meanwhile, the second composition with all percentages looks black, namely 5Y 2/1 (black). The color change in the second composition is caused by the mixing process and the distribution of material particles in the mixture, which can affect the final color. It can also be affected by exposure to different lights to make the color appear lighter or darker. The ameliorant composition between the two provides color changes that can occur due to variations in the types of organic and mineral compounds present in SC, and also those activated with NaOH. Meanwhile, B-YCW can change depending on the manufacturing process, including pyrolysis temperature and pyrolysis time, which can affect the color. Activation and pyrolysis processes, as well as different moisture content between the two materials, can also cause color changes in the blended materials [20].

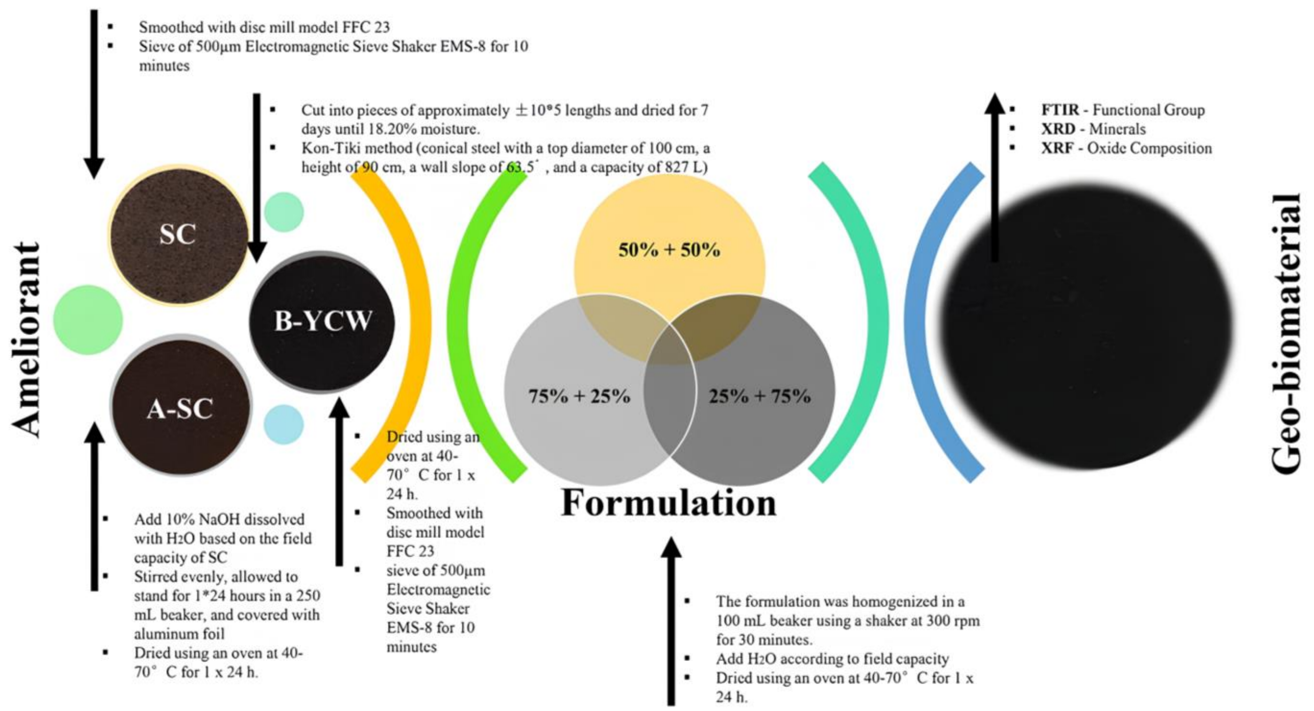

Figure 1. Geo-biomaterial production

3.1 Functional group from geo-biomaterial by FT-IR

The identification of functional groups from the ameliorant formulation between SC, A-SC, and B-YCW by FT-IR (Figure 2). FT-IR spectra of the ameliorant formulation showed the O-H or N-H groups at wavenumber 3336.63 - 3620.46 cm^{-1} with a transmittance of 86.77 - 92.82%. In the combination of SC + B-YCW, only at 75% + 25%, which produces O-H or N-H groups. While other percentages do not produce O-H or N-H groups. Different from the combination of A-SC + B-YCW, there is the appearance of O-H or N-H groups. This formulation shows that the lower the content of A-SC or the higher the content of B-YCW, the resulting transmittance decreases.

This indicates that there is an increase in absorption intensity or an increase in O-H or N-H groups, and shows that there is depolymerization (polymer disconnection) from the breakdown of SC molecules by NaOH to become more open and create more negative charges, and the presence of OH groups from B-YCW. The NaOH can play a role in depolymerizing coal molecules by breaking polymer bonds and opening up molecular structures. This process can lead to the release of O-H and N-H groups that were previously bound in the polymer structure. An increase in absorption intensity at these peaks in the FTIR results may reflect an increase in the number of such groups due to depolymerization. In addition, the presence of OH groups from the alkaline solution material (biochar or NaOH solution) may contribute to the increase in absorption intensity. The interaction between NaOH and coal and biochar can also cause chemical transformations that generate new OH groups, including hydroxyl groups involved in the opening of molecular structures. The opening of molecular structures and the release of OH or NH groups can result in more sites that can carry negative charges. This could indicate an increase in the negative charge on the coal surface. Thus, the process of depolymerization and breaking of polymer bonds can change the surface properties, making it more open and increasing its ability to capture or interact with OH groups from biochar [21].

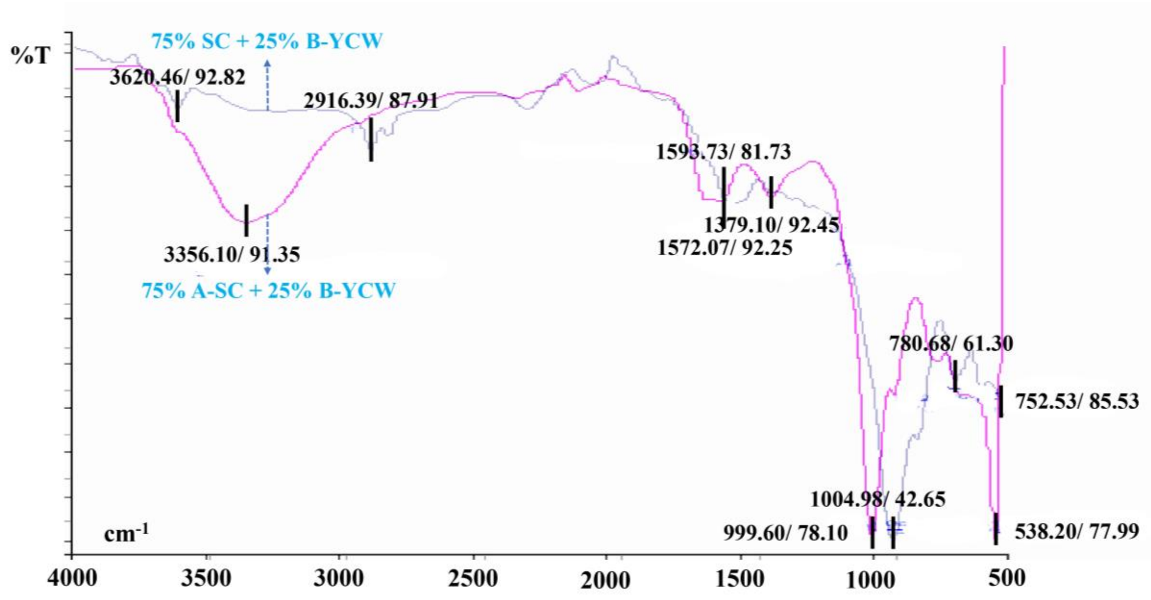

(A1)

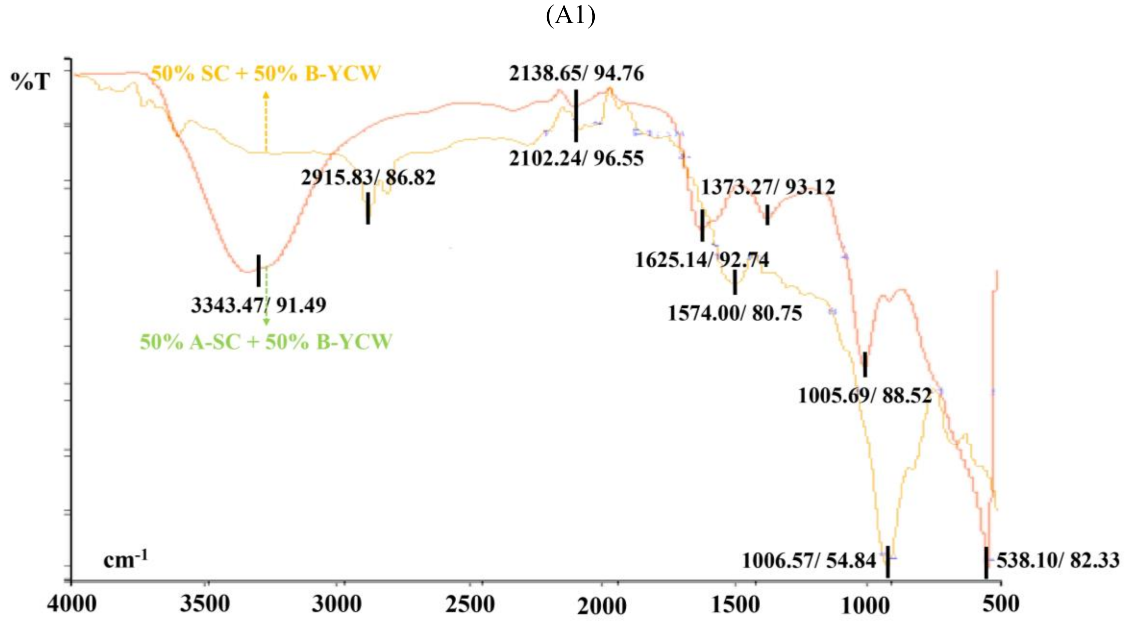

(A2)

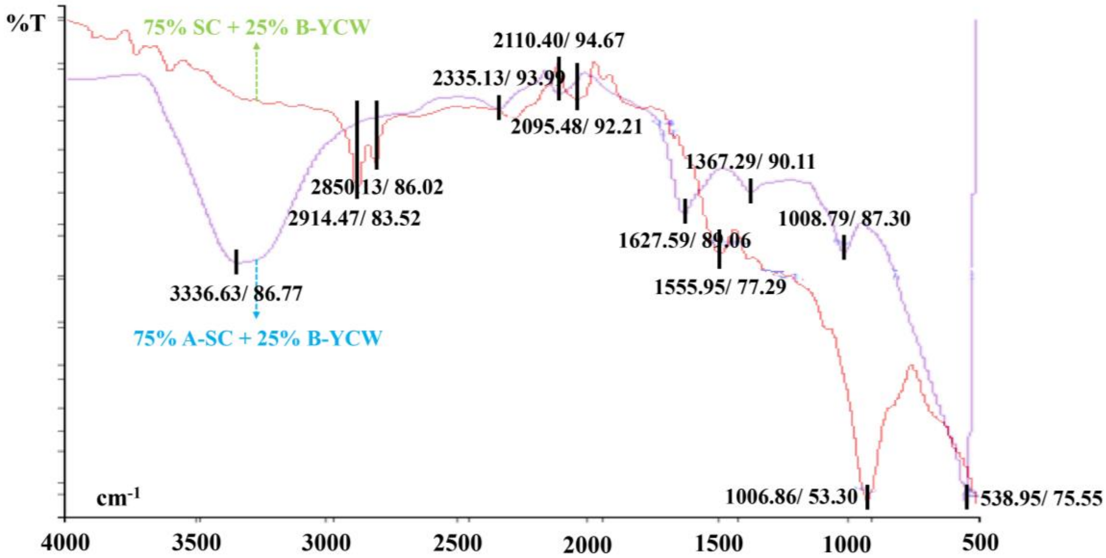

%T
75% SC + 25% B-YCW
2110.40/ 94.67
2335.13/ 93.99
2095.48/ 92.21
1367.29/ 90.11
2850.13/ 86.02
2914.47/ 83.52
1627.59/ 89.06
1008.79/ 87.30
3336.63/ 86.77
1555.95/ 77.29
75% A-SC + 25% B-YCW
cm-1
1006.86/ 53.30
538.95/ 75.55
4000
3500
3000
2500
2000
1500
1000
500

(A3)

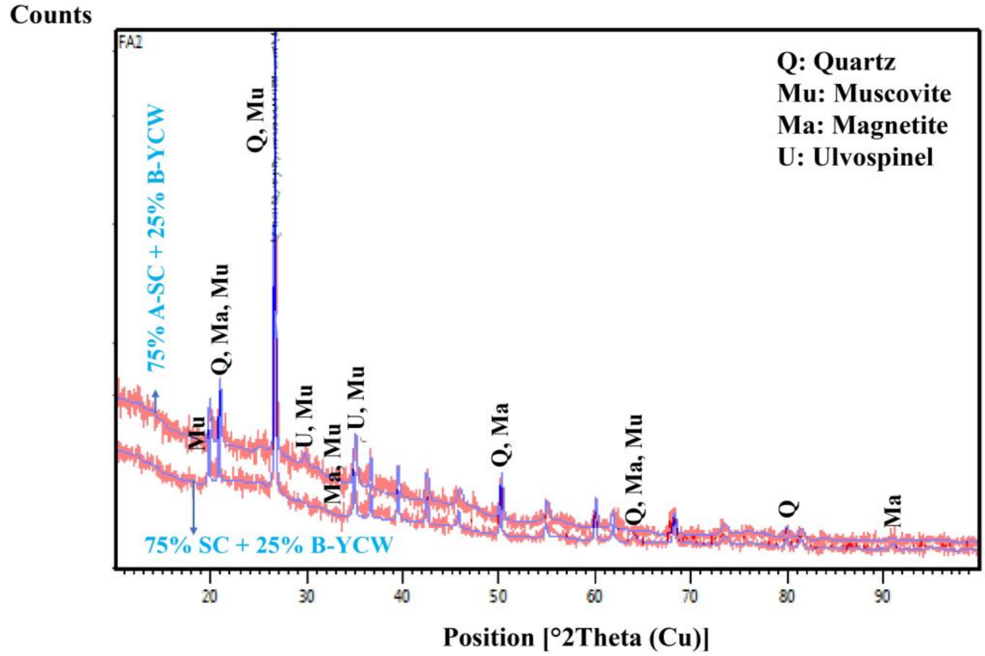

Counts
FA2
Q: Quartz
Mu: Muscovite
Ma: Magnetite
U: Ulvospinel
75% A-SC + 25% B-YCW
Q, Mu
Q, Ma, Mu
Mu
U, Mu
U, Mu
Ma, Mu
Q, Ma
Q, Ma, Mu
Q
Ma
75% SC + 25% B-YCW
20
30
40
50
60
70
80
90
Position [°2Theta (Cu)]

(B1)

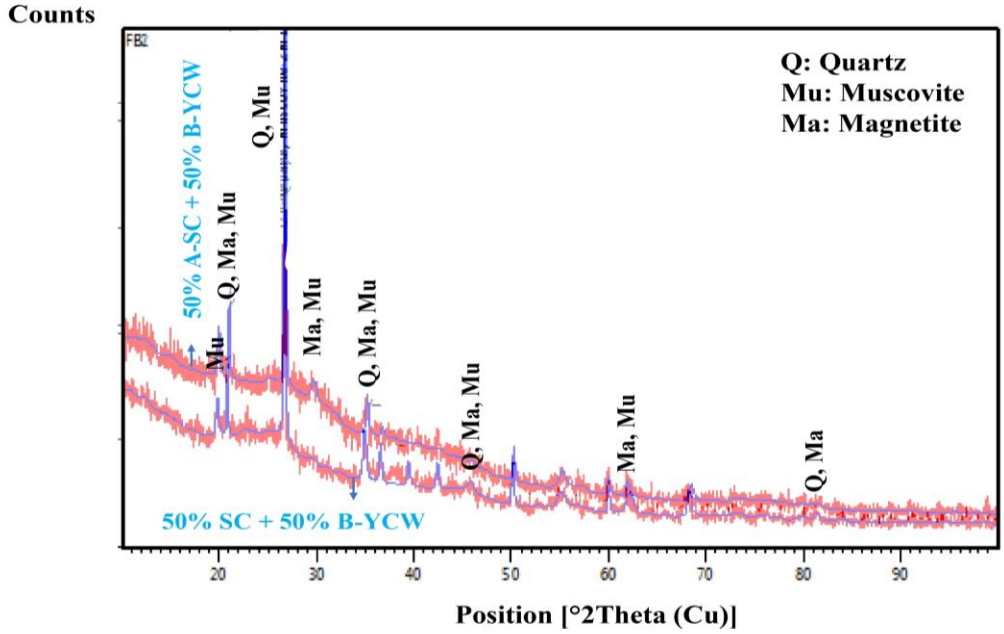

Counts
FB2
Q: Quartz
Mu: Muscovite
Ma: Magnetite
50% A-SC + 50% B-YCW
Q, Mu
Q, Ma, Mu
Mu
Ma, Mu
Q, Ma, Mu
Q, Ma, Mu
Ma, Mu
Q, Ma
50% SC + 50% B-YCW
20
30
40
50
60
70
80
90
Position [°2Theta (Cu)]

(B2)

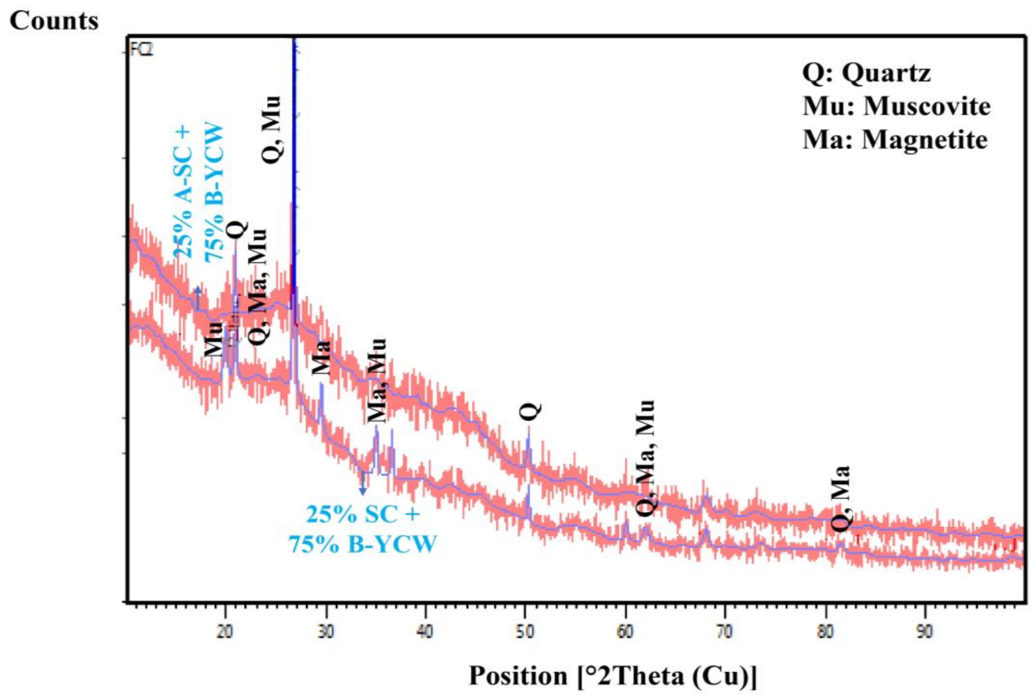

(B3)

Figure 2. The FT-IR (A) and XRD (B) of geo-biomaterial: (1) 75% + 25%; (2) 50% + 50%, and (3) 25% + 75%

The C-H stretching group of -C≡C-H; C=C-H was only found in the first combination at wavenumber 2850.13 - 2914.47 cm. A decrease in transmittance also occurred from 87.91 - 83.52%, where the higher the percentage of B-LKM content, or the decrease in SC composition in the formulation. This indicates that there is an increase in absorption intensity and an increase in -C≡C-H and C=C-H groups. Biochar contains organic compounds including -C≡C-H (alkynes) groups. During the pyrolysis process, bond breaking and decomposition of organic matter occur. Thus, the more molecular bonds that can be formed, will increase in absorption intensity will be. However, in contrast to the second combination, no C-H stretching groups of -C≡C-H and C=C-H were identified. The activation process with NaOH can involve depolymerization and bond-breaking in coal. NaOH has properties that can damage polymer structures and produce smaller and more reactive compounds, or absorption occurs between compounds on the surface of biochar with compounds produced during the activation process [22]. This can result in changes in chemical structure and the absence of -C≡C-H and C=C-H groups in the formulation.

The wavenumber 2095.48 - 2335.13 cm^{-1} shows C≡C; C≡N groups with transmittance levels at 90% in both ameliorant formulations. However, it was not found in the percentage of 75% SC + 25% B-YCW. It is suspected that coal and biochar have different chemical compositions and are formed through different processes, which may result in changes or loss of C≡C; C≡N functional groups. Different from the C=O stretching group, identified in all ameliorant formulations in both compositions. Biochar, which is created by the pyrolysis of organic materials with little oxygen, may contain C=O groups from organic molecules. Coal, on the other hand, which is formed through deposition and dissolution, can also contain C=O groups that may come from organic compounds decomposed during geological processes. The difference in chemical composition between coal and biochar can affect the intensity and uptake of C=O groups that can be derived from compounds such as ketones, aldehydes, or carboxylic acids [23].

The C-H stretching was only found in the second combination of A-SC + B-YCW, only at wavenumber 1367.29 - 1379.10 cm^{-1} with transmittance increasing at a percentage of 50% A-SC + 50% B-YCW and decreasing at a percentage of 25% A-SC + 75% B-YCW. This indicates an increase in C-H absorption intensity on decreasing the composition of coal activated with NaOH or on increasing the percentage of B-YCW. Activation with NaOH can change the coal structure and increase its hydrophobicity. The increase in hydrophobicity can be indicated by an increase in the intensity of C-H absorption. This activation may occur because NaOH can promote partial breakdown of organic matter in coal, increase the solubility of residual carbon, and cause the formation of more carbon bonds [24]. Biochar's hydrophobicity might indicate its capacity to hold water, and the interaction between biochar and C-H groups from coal activated with NaOH. Finally, the discovery of C=C-H contraction groups and mineral bonds at wave number 538.10 - 1008.79 cm^{-1} in all compositions and percentages of ameliorant formulations produced. Mineral bonds include absorption associated with chemical bonds involving certain minerals, such as metal oxides, silicates, and other mineral compounds [25].

The ameliorant formulations between SC, A-SC, and B-YCW showed different reactions on the surface oxy group composition (Figure 3). This suggests that the loading amount and/or sorption mechanism of the two interact with polar components via H-bonds, depleting numerous hydroxyl and carboxyl groups. The association of biochar with HA at 600°C can be through hydrophobic and π-π EDA (electron donor-acceptor) interactions because of its more hydrophobic surface, and graphite and π-π interactions are more important driving forces than surface O-functions in HA and biochar [26]. Thus, the relatively hydrophobic component of HA adsorbs on the carbon surface of biochar, leaving polar groups (e.g. hydroxyl and carboxyl groups) on the outer surface of the adlayer on HA, which causes the C=O groups of HA to possibly facilitate and/or be involved in the formation of EDA interactions between HA and biochar. This is also evidenced by the identification of functional groups of the ameliorant formulation in both compositions, where there is an increase in the peak intensity of the O-H (3428 cm^{-1}) and C=O (1072 cm^{-1}) groups in the ameliorant formulation, which has shifted the aromatic C=C and C=O bands. This explains the π-π EDA reaction between SC + B-YCW and A-SC + B-YCW.

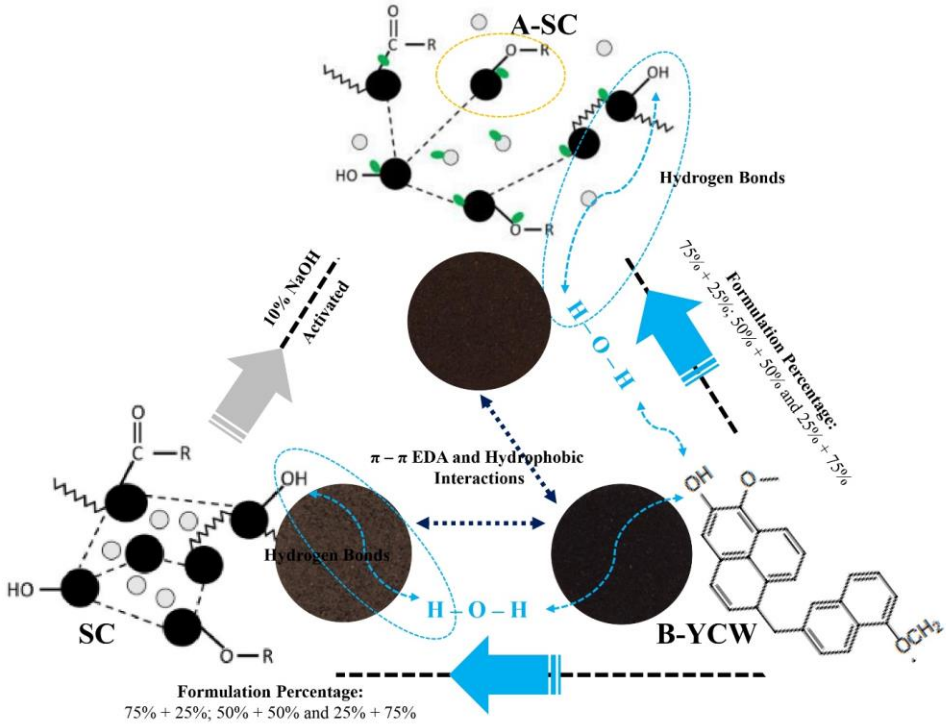

Figure 3. Mechanism prediction on the combination and percentage of ameliorant formulation on geo-biomaterials

3.2 Minerals from geo-biomaterial by XRD

The ameliorant formulation that was formed showed almost the same minerals in both combinations, and the percentage of ameliorant produced was quartz (SiO_2), muscovite ($Al_3H_2KO_{12}Si_3$), magnetite (Fe_3O_4), and ulvospinel (Fe_3O_4Ti) (Figure 2(B)). In the ameliorant formulation of SC + B-YCW, the minerals quartz, muscovite, and magnetite were identified in all three percentages used in the ameliorant formulation. Naturally, minerals such as quartz, muscovite, and magnetite are usually formed through geological processes under certain pressures and temperatures. The formation of such minerals involves complex natural conditions and takes place over very long periods. Coal is the result of the decay and accumulation of plant remains over millions of years, while biochar is the product of the pyrolysis of organic materials [27]. However, based on the XRF test, oxides of SiO_2, Al_2O_3, Fe_2O_3, and K_2O were identified in the ameliorant formulation SC + B-YCW. The most abundant mineral detected in the coal tested was quartz. This mineral is mainly of detrital origin [28]. The round-to-semi-round shape of quartz grains indicates that they were transported extensively before being deposited in the basin [29].

The same in the ameliorant formulation of A-SC + B-YCW identified quartz, magnetite, and muscovite minerals. However, the mineral ulvospinel was also identified at a percentage of 75% A-SC + 25% B-YCW, and a percentage of 25% A-SC + 75% B-YCW; only quartz was found. Coal is formed from plant remains that have undergone organic conversion under pressure and temperature for millions of years. The formation of certain minerals, such as ulvospinel, is generally related to geological conditions and processes that do not occur in the coal-forming environment. Activation of coal with NaOH can increase the reactivity of coal by the interaction between iron ions, titanium, and oxides in the activated coal and the formation of ulvospinel. NaOH activation causes the destruction of the carbon structure (graphitization) in coal. The formation of pores and increasing the specific surface area through the release of volatile compounds, increased carbon reactivity, and the formation of metal oxides through reactions with existing minerals (such as Fe_2O_3, TiO_2). NaOH increases the reactivity of Fe_2O_3 and TiO_2 through a strong base reaction, where ulvospinel (Fe_3O_4Ti) is formed as a recombination of iron and titanium in the spinel structure, which is stabilized by the base activation process [30]. Thus, NaOH as a base catalyst facilitates the reduction and recombination reactions of minerals in geo-biomaterials by increasing the contact between carbon and iron and titanium oxides and increasing the mobility of Fe and Ti ions to diffuse more easily to form the ulvospinel phase.

The 75% A-SC + 25% B-YCW identified the composition of Fe_2O_3 and TiO_2 oxides. Coal activation with NaOH can cause mineral alteration. NaOH is hypothesized to remove mineral layers and liberate metal ions such as Al and Ca into solution. This procedure may improve coal porosity and surface liveliness. The interaction of coal with NaOH can induce the elimination of K and Al ions, as well as impact the mineral structure and surface liveliness through changes in the coal's molecular structure, especially the organic portion [31, 32]. Quartz in biochar varies depending on the raw material.

The amount of quartz in biochar is determined by the biomass raw material utilized and the pyrolysis or carbonization processes. Biomass carbonization products, and during the process, most non-carbon elements (such as minerals and metals) can be decomposed or reduced [33]. This is thought to be most likely from the mineral components in the initial biomass.

3.3 Oxide composition from geo-biomaterial by XRF

The oxide composition of the ameliorant formulation in both combination types and ameliorant percentages was dominated by K_2O (45.65%); F_2O_3 (36.28%) and SiO_2 (32.80%) in the ameliorant formulation from SC + B-YCW and SiO_2 (45.08%); K_2O (31.82%) and CaO (28.46%) in the ameliorant formulation from A-SC + B-YCW (Figure 4). The ameliorant formulation of SC + B-YCW with a percentage of 75% SC + 25% B-YCW consists of the oxide composition P_2O_5; K_2O (11.07%); SO_3; CaO; ZnO; CuO; MnO; SiO_2 (45.08%); Cl; Fe_2O_3 (13.19%) and Al_2O_3 (13.81%). However, at a percentage of 50% SC + 50% B-YCW, no P_2O_5 and SiO_2 oxides were identified. While at a percentage of 75% SC + 25% B-YCW, both were identified again, but no Al_2O_3 oxide was identified. The oxide composition of the A-SC + B-YCW formulation consists of P_2O_5, K_2O (20.51%); CaO (17.62%); ZnO; CuO; MnO; Cl; Fe_2O_3 (36.28%), and Al_2O_3 (11.53%). Stable minerals include detrital minerals such as quartz, magnetite, mica, and muscovite. The ratio of these minerals in coal can remain almost constant, although their overall amount is strongly reliant on clastic material intake into the peat bog. This study's coal includes a larger amount of detrital minerals. It has been demonstrated that the number of detrital minerals in coal is increasing [34].

This oxide composition increased and decreased in the three percentages produced. At a percentage of 50% A-SC + 50% B-YCW, the P_2O_5 and Al_2O_3 oxides were not identified, but SiO_2 oxide was identified. Meanwhile, the percentage of 75% A-SC + 25% B-YCW did not identify SiO_2, P_2O_5, and Al_2O_3 oxides again, but SO_3 oxide was identified. Oxide composition decreased and increased in some oxides from the ameliorant formulation results. It is suspected that the interaction between coal and biochar in the mixture can affect oxide emissions. The process of increasing oxides can occur if the coal used contains more identified elements. Biochar produced from biomass through the pyrolysis process can also affect oxide formation. NaOH may alter the oxide content of coal. The interaction between NaOH, biochar, and coal can result in the production of some oxides and change the shape of existing oxides.

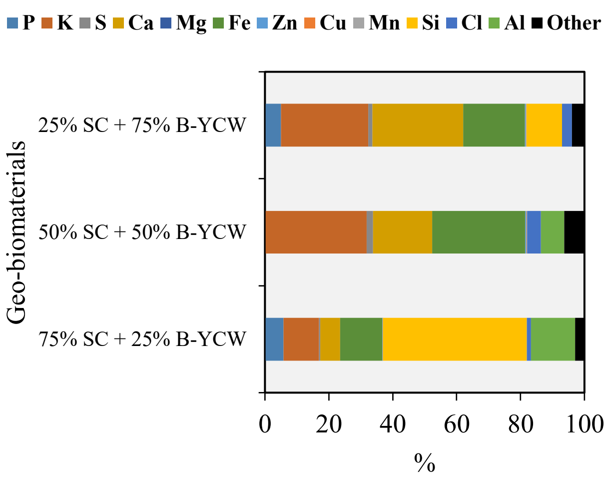

(A)

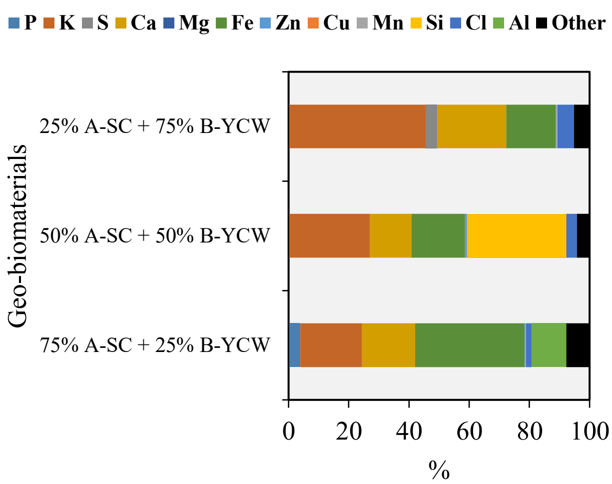

(B)

Figure 4. Oxide composition of ameliorant formulation from (A) SC + B-YCW and (B) A-SC + B-YCW by XRF

Chemical activation can accelerate the creation of carbon oxides, such as carbonates and bicarbonates. The organic percentage of coal, as well as the carbon oxides produced, can contribute to a rise in coal pH. The A-SC's pH increased by 12.60 units. NaOH may liberate ions such as silicon, aluminium, and calcium into solution, affecting the structure and solubility of iron oxides in coal [35]. Calcite minerals in biochar are strongly influenced by the biomass feedstock used and the conditions of the pyrolysis or carbonization process. The carbonization process can affect the transformation of minerals in biomass into biochar. At high temperatures during the pyrolysis process, most of the non-carbon components in biomass, including minerals, can undergo decomposition or transformation [36]. Biomass of young coconut waste contains oxide composition K_2O (33.59%) > CaO (21.66%), after the pyrolysis process, oxide composition K_2O (32.73%) < CaO (33.37%) [14, 15].

The increase of oxides such as CaO, K_2O, SO_3, and additional elements such as CuO and Cl in geo-biomaterials has significant potential to be used as fertilizer substitutes or supplements. CaO is a source of calcium, which is important for plant cell wall strength and neutralization of soil acidity (pH increase) as a soil limiter, especially on acidic soils [37]. Meanwhile, K_2O oxide is a source of potassium, which is important for protein formation, osmotic regulation, and increased resistance to abiotic stress for plants that require high potassium, such as fruit crops [38]. However, SO_3 oxide in the soil will form sulfate (SO_4^{2-}), which is important for protein synthesis and enzyme formation and provides an additional source of sulfur, which is beneficial for crops that require high sulfur, such as legumes [39]. Meanwhile, CuO oxide provides the microelement copper, which is important for photosynthesis and lignin formation [40]. On the other hand, Cl is required in small amounts for photosynthesis, regulation of osmotic pressure, and enhancing plant resistance to drought, but it should be noted that high chloride levels can be toxic to some plants [41]. This proves that geo-biomaterials have great potential as multi-nutrient fertilizers, especially in increasing potassium and calcium content. However, the chloride content is high, so care should be taken with salt-sensitive crops.

4. CONCLUSIONS

The ameliorant formulations from geo-biomaterials identified functional groups [O-H; N-H; C-H; -C≡C-H; C=C-H; C≡C; C≡N; C=O; C-H; C=C-H and minerals (quartz, muscovite, magnetite and ulvospinel)] and oxide composition (P_2O_5; K_2O; SO_3; CaO; MgO; ZnO; CuO; MnO; SiO_2; Cl; Fe_2O_3 and Al_2O_3). Formulations of 25% SC+75% B-YCW and 25% A-SC+75% B-YCW showed a decrease in transmittance towards stretching of C-H groups from -C≡C-H; C=C-H and shrinking of -C-H groups. Meanwhile, the oxide content of CaO increased from 6.23% to 28.46% (25% SC+75% B-YCW) and K_2O from 20.51% to 45.65%; SO_3 from 0 to 3.58%; CaO from 13.85% to 23.03%; CuO from 0.08% to 0.13%; Cl from 1.84% to 5.59% (25% A-SC+75% B-YCW), compared to the other formulations. The ameliorant formulation of 25% SC+75% B-YCW or 25% A-SC+75% B-YCW can be recommended as a soil ameliorant.

ACKNOWLEDGMENT

The authors would like to thank Andalas University for supporting this research with contract No.: 375//UN16.19/PT.01.03/PUJK/2024.

REFERENCES

[1] Pandian, K., Mustaffa, M.R.A.F., Mahalingam, G., Paramasivam, A., Prince, A.J., Gajendiren, M., Rafiqi Mohammad, A.R., Varanasi, S.T. (2024). Synergistic conservation approaches for nurturing soil, food security and human health towards sustainable development goals. Journal of Hazardous Materials Advances, 16: 100479. https://doi.org/10.1016/j.hazadv.2024.100479

[2] Chen, Q., Song, Y., An, Y., Lu, Y., Zhong, G. (2024). Soil microorganisms: Their role in enhancing crop nutrition and health. Diversity, 16(12): 734. https://doi.org/10.3390/d16120734

[3] Herviyanti, H., Gusnidar, G., Harianti, M., Maulana, A. (2019). Improvement Chemical Properties of Oxisols and Rice Production with Humic Substances from Sub-bituminous Coal Indonesia. AGRIVITA Journal of Agricultural Science, 41(3): 428-438. https://doi.org/10.17503/agrivita.v41i3.1106

[4] Herviyanti, H., Gusnidar, G., Harianti, M. (2013). Using of humic matter from low rank coal to increase phosphorous fertilizer efficiency and production of corn at oxisol. International Journal on Advanced Science, Engineering and Information Technology, 3(5): 350-354. https://doi.org/10.18517/ijaseit.3.5.340

[5] Rezki, D., Ahmad, F., Gusnidar, G. (2007). Ekstraksi bahan humat dari batubara (Subbituminus) dengan menggunakan 10 jenis pelarut. Jurnal Solum, 4(2): 73-80. https://doi.org/10.25077/js.4.2.73-80.2007

[6] Herviyanti, H., Maulana, A., Pasetyo, T.B., Omily, T., Ryswaldi, R. (2021). Application of sub-bituminous coal activated with urea to improve chemical properties of ultisols and palm oil's growth (Elaeis Guineensis Jacq.) in Pulau Punjung, Dharmasraya. International Journal on Advanced Science, Engineering and Information Technology, 11(2): 791-797. https://doi.org/10.18517/ijaseit.11.2.13536

[7] Herviyanti, H., Maulana, A., Prasetyo, T.B., Darfis, I., Hakim, L., Ryswaldi, R. (2021). Activation of sub-bituminous coal with dolomite to improve chemical properties and palm oil growth on ultisols. IOP Conference Series: Earth and Environmental Science, 741(1): 012032. https://doi.org/10.1088/1755-1315/741/1/012032

[8] Prasetyo, T. B., Harianti, M., Panjaitan, N. P. (2018). Activation of sub-bituminous powder with urea and dolomite to improve nutrient content of ultisols and the growth of oil palm [Elaeis guineensis Jacq] Seedlings. Malaysian Journal of Soil Science, 22: 147-160.

[9] Garcia, D., Cegarra, J., Bernal, M.P., Navarro, A. (1993). Comparative evaluation of methods employing alkali and sodium pyrophosphate to extract humic substances from peat. Communications in Soil Science and Plant Analysis, 24(13-14): 1481-1494. https://doi.org/10.1080/00103629309368893

[10] Cheng, G., Niu, Z., Zhang, C., Zhang, X., Li, X. (2019). Extraction of humic acid from lignite by KOH-hydrothermal method. Applied Sciences, 9(7): 1356. https://doi.org/10.3390/app9071356

[11] Torrecillas, C., Martínez-Sabater, E., Gálvez-Sola, L., et al. (2013). Study of the organic fraction in biosolids. Communications in Soil Science and Plant Analysis, 44(1-4): 492-501. https://doi.org/10.1080/00103624.2013.744150

[12] Li, Y., Yuan, S. (2021). Influence of addition of KOH on the yield and characteristics of humic acids extracted from lignite using NaOH. SN Applied Sciences, 3: 1-10. https://doi.org/10.1007/s42452-020-04087-x

[13] Herviyanti, H., Prasetyo, T.B., Juniarti, J., Prima, S., Wahyuni, S. (2018). The role of powder sub-bituminous coal with sodium hydroxide (NaOH) to improve chemical properties of ultisols. International Journal of Advanced Science Engineering Information Technology, 8(5): 2052-2058. https://doi.org/10.18517/ijaseit.8.5.3543

[14] Lita, A.L., Maulana, A., Ryswaldi, R. (2022). Characteristics biochar from young coconut waste based on particle size as améliorant. IOP Conference Series: Earth and Environmental Science, 959(1): 012034. https://doi.org/10.1088/1755/1315/959/1/012034

[15] Maulana, A., Prasetyo, T.B., Harianti, M., Lita, A.L. (2022). Effect of pyrolysis methods on characteristics of biochar from young coconut waste as ameliorant. IOP Conference Series: Earth and Environmental Science, 959(1): 012035. https://doi.org/10.1088/1755/1315/959/1/012035

[16] Herviyanti, H., Maulana, A., Prima, S., Aprisal, A., Crisna, S.D., Lita, A.L. (2020). Effect of biochar from young coconut waste to improve chemical properties of ultisols and growth coffee [*Coffea arabica* L.] plant seeds. IOP Conference Series: Earth and Environmental Science, 497(1): 012038. https://doi.org/10.1088/1755-1315/497/1/012038

[17] Darfis, I., Maulana, A., Fathi, A.N.M., Rezki, D., Junaidi,

J., Herviyanti, H. (2023). The effect of pyrolysis methods and particle size on biochar characteristics of Surian (*Toona ciliata*) as ameliorant. AIP Conference Proceedings, 2730(1): 120002. https://doi.org/10.1063/5.0127751

[18] Herviyanti, Prasetyo, T.B., Maulana, A., Lita, A.L., Ryswaldi, R. (2022). Characteristics of biochar methods from bamboo as améliorant. IOP Conference Series: Earth and Environmental Science, 959: 012036. https://doi.org/10.1088/1755-1315/959/1/012036

[19] Singh, B., Camps-Arbestain, M., Lehmann, J. (2017). Biochar: A Guide to Analytical Methods. Csiro Publishing.

[20] Chew, T.W., H'Ng, P.S., Luqman Chuah Abdullah, B. C.T.G., Chin, K.L., Lee, C.L., Mohd Nor Hafizuddin, B.M.S., TaungMai, L. (2023). A review of bio-based activated carbon properties produced from different activating chemicals during chemicals activation process on biomass and its potential for Malaysia. Materials, 16(23): 7365. https://doi.org/10.3390/ma16237365

[21] Ma, H., Zhu, H., Yi, C., Fan, J., Chen, H., Xu, X., Wang, T. (2019). Preparation and reaction mechanism characterization of alkali-activated coal gangue–slag materials. Materials, 12(14): 2250. https://doi.org/10.3390/ma12142250

[22] Tseng, R.L. (2006). Mesopore control of high surface area NaOH-activated carbon. Journal of Colloid and Interface Science, 303(2): 494-502. https://doi.org/10.1016/j.jcis.2006.08.024

[23] Akpasi, S.O., Anekwe, I.M.S., Adedeji, J., Kiambi, S.L. (2022). Biochar development as a catalyst and its application. In Biochar-Productive Technologies, Properties and Applications. IntechOpen, 11: 28. https://doi.org/10.5772/intechopen.105439

[24] Lei, Z., Liu, M., Shui, H., Wang, Z., Wei, X. (2010). Study on the liquefaction of Shengli lignite with NaOH/methanol. Fuel Processing Technology, 91(7): 783-788. https://doi.org/10.1016/j.fuproc.2010.02.014

[25] Goff, J.P. (2018). *Invited review*: Mineral absorption mechanisms, mineral interactions that affect acid–base and antioxidant status, and diet considerations to improve mineral status. Journal of Dairy Science, 101(4): 2763-2813. https://doi.org/10.3168/jds.2017-13112

[26] Lian, F., Sun, B., Chen, X., Zhu, L., Liu, Z., Xing, B. (2015). Effect of humic acid (HA) on sulfonamide sorption by biochars. Environmental Pollution, 204: 306-312. https://doi.org/10.1016/j.envpol.2015.05.030

[27] Palin, R.M. (2022). Metamorphism and its bearing on geosystems. Geosystems and Geoenvironment, 1(1): 100012. https://doi.org/10.1016/j.geogeo.2021.100012

[28] Bishop, B.A., Shivakumar, K.R., Alessi, D.S., Robbins, L.J. (2023). Insights into the rare earth element potential of coal combustion by-products from western Canada. Environmental Science: Advances, 2(3): 529-542. https://doi.org/10.1039/D2VA00310D

[29] Gopinathan, P., Subramani, T., Barbosa, S., Yuvaraj, D. (2023). Environmental impact and health risk assessment due to coal mining and utilization. Environmental Geochemistry and Health, 45(10): 6915-6922. https://doi.org/10.1007/s10653-023-01744-z

[30] Blanco, M.V., Abdala, P.M., Gennari, F., Cova, F. (2021). Dynamics of phase transitions in Na_2TiO_3 and its possible utilization as a CO_2 sorbent: A critical analysis. Reaction Chemistry & Engineering, 6(10): 1974-1982. https://doi.org/10.1039/D1RE00125F

[31] Acevedo, S., Galicia, L., Plaza, E., Atencio, R., Rodríguez, A., González, E. (2016). Activated carbon prepared from bituminous coal with potassium hydroxide activation. Revista Técnica de la Facultad de Ingeniería Universidad del Zulia, 39(2): 064-070.

[32] Kim, S., Lee, S.E., Baek, S.H., Choi, U., Bae, H.J. (2023). Preparation of activated carbon from Korean anthracite: Simultaneous control of ash reduction and pore development. Processes, 11(10): 2877. https://doi.org/10.3390/pr11102877

[33] Hamissou, I.G.M., Appiah, K.E.K., Sylvie, K.A.T., Ousmaila, S.M., Casimir, B.Y., Kouassi Benjamin, Y. (2023). Valorization of cassava peelings into biochar: Physical and chemical characterizations of biochar prepared for agricultural purposes. Scientific African, 20: e01737. https://doi.org/10.1016/j.sciaf.2023.e01737

[34] Dai, S., Finkelman, R.B., French, D., Hower, J.C., Graham, I.T., Zhao, F. (2021). Modes of occurrence of elements in coal: A critical evaluation. Earth-Science Reviews, 222: 103815. https://doi.org/10.1016/j.earscirev.2021.103815

[35] Wiśniewska, M., Sadłowska, A., Herda, K., Urban, T., Nowicki, P. (2023). Production of mineral-carbon composites and activated carbons as a method of used gear oil, ashes, and low-quality brown coals management. Molecules, 28(19): 6919. https://doi.org/10.3390/molecules28196919

[36] Hu, Z., Wei, L. (2023). Review on characterization of biochar derived from biomass pyrolysis via reactive molecular dynamics simulations. Journal of Composites Science, 7(9): 354. https://doi.org/10.3390/jcs7090354

[37] Husain, S.H., Mohammed, A., Ch'ng, H.Y., Khalivulla, S.I. (2021). Residual effects of calcium amendments on oil palm growth and soil properties. IOP Conference Series: Earth and Environmental Science, 756(1): 012060. https://doi.org/10.1088/1755 1315/756/1/012060

[38] Wang, Q., Shan, C., Zhang, P., Zhao, W., Zhu, G., Sun, Y., Wang, Q., Jiang, Y., Shakoor, N., Rui, Y. (2024). The combination of nanotechnology and potassium: Applications in agriculture. Environmental Science and Pollution Research, 31(2): 1890-1906. https://doi.org/10.1007/s11356-023- 31207-y

[39] Narayan, O.P., Kumar, P., Yadav, B., Dua, M., Johri, A.K. (2023). Sulfur nutrition and its role in plant growth and development. Plant Signaling & Behavior, 18(1): 2030082. https://doi.org/10.1080/15592324.2022.2030082

[40] Mahawar, L., Živčák, M., Barboricova, M., Kovár, M., Filaček, A., Ferencova, J., Vysoká, D.M., Brestič, M. (2024). Effect of copper oxide and zinc oxide nanoparticles on photosynthesis and physiology of *Raphanus sativus* L. under salinity stress. Plant Physiology and Biochemistry, 206: 108281. https://doi.org/10.1016/j.plaphy.2023.108281

[41] Colmenero-Flores, J.M., Franco-Navarro, J.D., Cubero-Font, P., Peinado-Torrubia, P., Rosales, M.A. (2019). Chloride as a beneficial macronutrient in higher plants: New roles and regulation. International Journal of Molecular Sciences, 20(19): 4686. https://doi.org/10.3390/ijms20194686